Convergence of a cartesian method for elliptic problems with immersed interfaces

Lisl Weynans

Convergence of a cartesian method for elliptic problems with immersed interfaces

L. Weynans[1]

[1]**Team Memphis, INRIA Bordeaux-Sud-Ouest & CNRS UMR 5251, Université de Bordeaux, France**

RESEARCH REPORT

N° 8872

Mars 2016

Project-Teams Memphis

ISSN 0249-6399 ISRN INRIA/RR--8872--FR+ENG

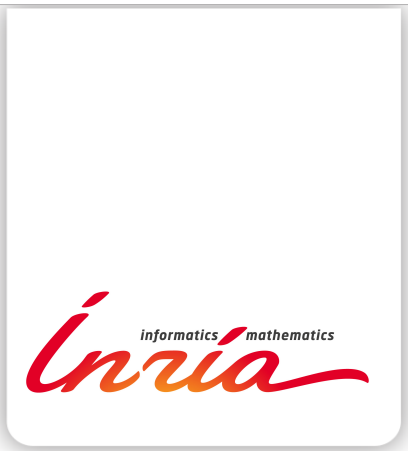

Convergence of a cartesian method for elliptic problems with immersed interfaces

L. Weynans[1]*

[1]Team Memphis, INRIA Bordeaux-Sud-Ouest & CNRS UMR 5251,
Université de Bordeaux, France

Project-Teams Memphis

Research Report n° 8872 — Mars 2016 — 20 pages

Abstract: We study in this paper the convergence of a cartesian method for elliptic problems with immersed interfaces that was introduced in a previous paper [8]. This method is based on additional unknowns located on the interface, that are used to discretize separately the elliptic operator in each subdomain and to express the jump conditions across the interface. It was shown numerically to converge with second-order accuracy in L^∞-norm. This paper is a step toward the convergence proof of this method. Indeed, we prove the convergence of the method in two cases: the original second-order method in one dimension, and a first-order version in two dimensions. This first-order version is based on the same ideas as the original method, but the discretization of the normal derivatives across the interface has only a first-order truncation error, instead of a second-order for the original method. The proof of convergence is in both cases inspired from the paper of Ciarlet [7] and takes advantage of a discrete maximum principle to obtain estimates on the coefficients of the inverse matrix.

Key-words: Finite-differences, cartesian method, elliptic problem, interface discontinuity, interface unknowns, discrete Green's function, convergence

* Corresponding author: lisl.weynans@inria.fr

RESEARCH CENTRE
BORDEAUX – SUD-OUEST

351, Cours de la Libération
Bâtiment A 29
33405 Talence Cedex

Convergence d'une méthode cartésienne pour des problèmes elliptiques avec interfaces immergées

Résumé : Nous étudions dans ce rapport la convergence d'une méthode sur grille cartésienne pour des problèmes elliptiques avec des interfaces immergées, introduite dans [8]. Cette méthode repose sur l'utilisation d'inconnues supplémentaires situées sur l'interface, qui servent à discrétiser séparément l'opérateur elliptique dans chaque sous-domaine et à exprimer avec une précision suffisante les conditions de saut au travers de l'interface. Il a été montré numériquement dans [8] que cette méthode converge à l'ordre deux en norme L^∞. Cet article est un pas en avant vers la preuve de la convergence à l'ordre deux de cette méthode. En effet, nous prouvons la convergence dans deux cas: celui de la méthode originale en une dimension, et celui d'une version à l'ordre un, mais en deux dimensions. Cette version à l'ordre un repose sur les mêmes idées que la méthode originale mais la discrétisation des dérivées normales au travers de l'interface a seulement une erreur de troncature d'ordre un, au lieu de l'ordre deux pour la méthode originale. La preuve de convergence est dans les deux cas inspirée du papier de Ciarlet [7], et tire profit d'un principe du maximum discret pour obtenir des estimations des coefficients de la matrice inverse.

Mots-clés : Différences finies, problème elliptique, méthode cartésienne, discontinuité au travers de l'interface, inconnues sur l'interface, fonction de Green discrète, convergence

Contents

1 Introduction

In this paper we aim to study the convergence of a method developed in a previous paper [8] to solve on a cartesian grid the following problem elliptic problem, defined on a domain Ω consisting in the union of two subdomains Ω_1 and Ω_2, separated by a complex interface Σ (see Figure 1):

$$-\nabla.(k\nabla u) = f \text{ on } \Omega = \Omega_1 \cup \Omega_2 \tag{1}$$

$$[\![u]\!] = \alpha \text{ on } \Sigma \tag{2}$$

$$[\![k\frac{\partial u}{\partial n}]\!] = \beta \text{ on } \Sigma \tag{3}$$

with k constant on each subdomain Ω_1 and Ω_2, assorted with boundary conditions on $\delta\Omega$ defined as the boundary of Ω, and where $[\![\cdot]\!]$ means $\cdot_1 - \cdot_2$. We assume, by convention, that the coefficient k is larger in Ω_2 than in Ω_1, and that the vector $\mathbf{n}$ is the outside normal for the subdomain Ω_2. Note that others configurations than the one illustrated on this figure are possible, for instance, Ω_1 separated in several subdomains, and are all covered by our analysis.

This elliptic problem with discontinuities across an interface appears in numerous physical or biological models. Among the well-known applications are heat transfer, electrostatics, incompressible flows with discontinuous densities and viscosities [2], but similar elliptic problems arise for instance in tumour growth modelling, where one has to solve a pressure equation [4], or in the modelling of electric potential in biological cells: see for instance [5] and [12].

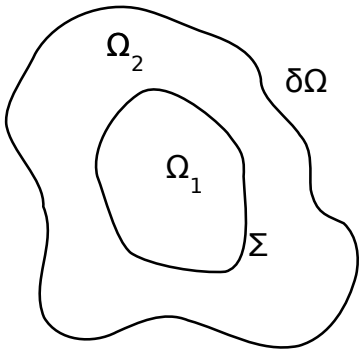

Figure 1: Geometry considered: two subdomains Ω_1 and Ω_2 separated by a complex interface Σ.

The method that we study is based on a finite-difference discretization and a dimension by dimension approach. In order to solve accurately the problem defined by equations (1) - (3) near the interface, additional unknowns are defined at the intersections of the interface with the grid, see Figure 2. These interface unknowns are used in the discretization of the elliptic operator near the interface, and avoid us to derive specific finite differences formulas containing jump terms, corrective terms, or needing the inversion of a linear system, as in many other second-order Cartesian methods. In order to solve the interface unknowns, the flux jump conditions are discretized and added to the linear system to solve. Jump conditions and the coupling of the solution in the different subdomains are thus handled independently of the discretization of the elliptic equation.

Here we will prove the convergence of the method in two cases: the original second-order method in one dimension, and a first-order version in two dimensions. This first-order version is based on the same

ideas as the original method, but the discretization of the normal derivatives across the interface has only a first-order truncation error, instead of a second-order for the original method.

The proof of convergence is based on the monotonicity of the discretization matrix. Note that this monotonicity is not trivial for the second-order discretization, since the discretization matrix is not diagonally dominant, due to the discretization of the flux jump conditions across the interface. Once it is proven that this matrix is monotone, then it is possible to obtain accurate estimates of the coefficients of the inverse matrix, block by block, in order to account for the different types of truncation errors, thanks to a technique presented in [7]. Combined to the truncation error coefficients block by block, these estimates provide first- or second-order bounds on the error between the exact and the numerical solution.

The first-order convergence in two dimensions can be considered as a result in itself, but we mainly consider it as a first step for the study of the convergence of the original second-order method in two dimensions. However the technique that we use to prove the convergence could also be useful to prove the convergence of other finite-difference methods for elliptic problems with discontinuities across interfaces. In the whole paper, we assume that the source term f is such that the solution u exists and is smooth enough so that our truncation error analyses are valid.

2 Description of the numerical schemes

2.1 Interface representation and classification of grid points

The problem (1) - (3) is discretized on a uniform cartesian grid covering $\Omega_1 \cup \Omega_2$, see Figure 3. The grid spacing is denoted h. The points on the cartesian grid are named either with letters such as P or Q, or with indices such as $M_{i,j} = (x_i, y_j) = (ih, jh)$ if one needs to have informations about the location of the point. We denote by u_{ij} the approximation of u at the point (x_i, y_j).

In order to describe accurately the geometric configuration in the vicinity of the interface we use the level set method introduced by Osher and Sethian [19]. We refer the interested reader to [20], [21] and [18] for recent reviews of this method. The zero isoline of the level set function, defined by the signed function φ:

$$\varphi(x) = \begin{cases} dist_\Sigma(x) & \text{outside of the interface} \\ -dist_\Sigma(x) & \text{inside of the interface} \end{cases} \tag{4}$$

represents implicitely the interface Σ immersed in the computational domain.

We assume that the interface is smooth enough, so that the derivatives of the level-set function in the vicinity of the interface are well-defined. A useful property of the level set function is

$$\mathbf{n}(x) = \frac{\nabla\varphi(x)}{|\nabla\varphi(x)|}, \tag{5}$$

where $\mathbf{n}(x)$ is the outward normal vector of the isoline of φ passing on x. This allows us to compute the values of the normal to the interface. In this paper, the level-set is defined so that $\mathbf{n}$ is the outside normal for the subdomain Ω_2.

We say that a grid point is irregular if it is neighbouring the interface, that is, if the sign of φ changes between this point and at least one of its neighbours, see Figure 2. On the contrary, grid points that are not irregular are said regular grid points. The set of grid points located inside the domain Ω is denoted Ω_h. The set of regular grid nodes is denoted Ω_h^{**}, and the set of irregular grid nodes is denoted Ω_h^*. The set of of points located at the intersection of the axes of the grid and the interface Σ, which are called the interface points, is denoted Σ_h, see Figure 3 for an illustration. These points are used to impose the boundary conditions in the numerical scheme. We also denote $\delta\Omega_h$ the set of points defined as the intersection between the grid and $\delta\Omega$. They are used to impose boundary conditions.

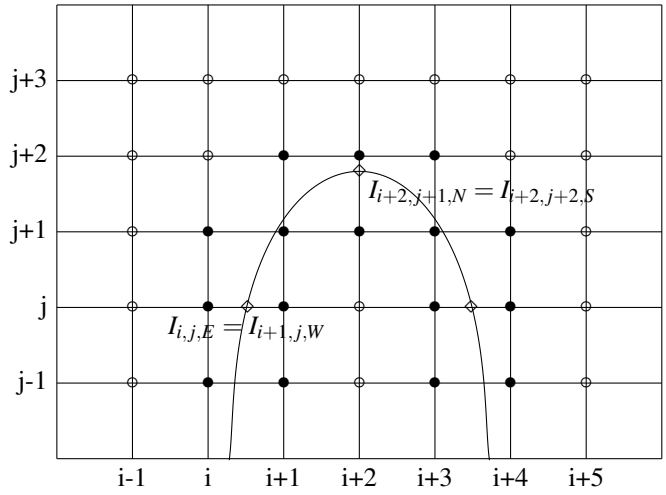

Figure 2: Example of geometrical configuration, with regular grid points (belonging to Ω_h^{**} in black, irregular points (belonging to Ω_h^*) in white, and interface points (belonging to Σ_h) with the two possible notations.

We define the interface point $I_{i,j,\mathrm{E}} = (\tilde{x}_{i,j,\mathrm{E}}, y_j)$ as the intersection of the interface and the segment $[M_{ij}M_{i+1\,j}]$, if it exists. In the same way, if the intersection of the interface and $[M_{i-1\,j}M_{ij}]$ exists, then we define the interface point $I_{i,j,\mathrm{W}} = (\tilde{x}_{i,j,\mathrm{W}}, y_j)$ as this intersection. Similarly, the interface points $I_{i,j,\mathrm{N}} = (x_i, \tilde{y}_{i,j,\mathrm{N}})$ and $I_{i,j,\mathrm{S}} = (x_i, \tilde{y}_{i,j,\mathrm{S}})$ are respectively defined as the intersection of the interface and the segments $[M_{ij}M_{ij+1}]$ and $[M_{ij-1}M_{ij}]$. Let us remark that, with this notation, the same interface point is described in two different ways: for instance

$$I_{i,j,\mathrm{S}} = I_{i,j-1,\mathrm{N}} \text{ or } I_{i,j,\mathrm{E}} = I_{i+1,j,\mathrm{W}}.$$

At each interface point we create two additional unknowns, called interface unknowns, and denoted by $\tilde{u}_{i,j,\gamma}$ with $\gamma = \mathrm{E}, \mathrm{W}, \mathrm{N}$ or S. The interface unknowns carry the values of the numerical solution on each side of the interface.

2.2 Second-order discretization in one dimension

We briefly recall the one-dimensional version of the numerical scheme that was introduced in [8] .

- Discrete elliptic operator on a grid point M_i

  We use the standart three point stencil: M_i and its nearest neighbors in each direction, either grid points or interface points. More precisely, we denote u_E the value of the solution on the nearest point in the east direction, and x_E its coordinate. Similarly, we define u_W the value of the solution on the nearest point in the west direction, and x_w its coordinate. The discretization at point x_i reads

$$-\Big(\nabla.(\nabla u)\Big)_i \quad = \quad \frac{2}{x_E - x_W}\Big(\frac{u_E - u_i}{x_E - x_i} - \frac{u_i - u_W}{x_i - x_W}\Big). \tag{6}$$

  The truncation error of this discretization is second-order accurate if all the points involved are grid points, and first-order otherwise.

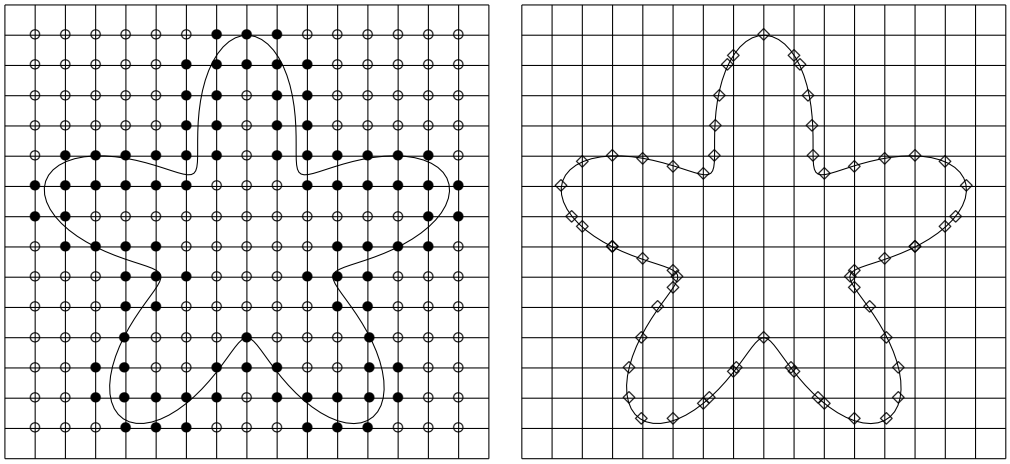

Figure 3: Left: regular nodes (belonging to Ω_h^{**}) described by bullets $\bullet$, irregular nodes (belonging to Ω_h^{**}) described by circles $\circ$:, right: nodes belonging to Σ_h.

- Discrete jump conditions across the interface

  On Figure 4, we present a prototypical situation around the interface: the interface point $x_{int} = \tilde{x}_{k,E}$ is located between the grid points x_k and x_{k+1} and we denote $dh = x_{k+1} - x_{int}$. We assume for instance that the subdomain Ω_2 is located on the left side of the interface, and Ω_1 on the right side. The normal to the interface is oriented from the left to the right.

  The left and right normal derivatives at the interface are computed with second order formulas using three non equidistant points:

$$\begin{aligned}(\partial_n u^1)_{int} &= \frac{1+2d}{d(d+1)h}(u_{k+1} - \tilde{u}^1_{k,E}) - \frac{d}{(1+d)h}(u_{k+2} - u_{k+1}),\\ (\partial_n u^2)_{int} &= \frac{3-2d}{(1-d)(2-d)h}(\tilde{u}^2_{k,E} - u_k) - \frac{1-d}{(2-d)h}(u_k - u_{k-1}).\end{aligned}$$

  We express the jump conditions at point x_L as

$$k_2(\partial_n u^2)_{x_{int}} - k_1(\partial_n u^1)_{x_{int}} = \beta(x_{int}), \quad (7)$$

$$\tilde{u}^2_{k,E} - \tilde{u}^1_{k,E} = \alpha(x_{int}). \quad (8)$$

2.3 First-order discretization in two dimensions

The numerical solution is obtained by solving the linear system arising from the following equations:

- Discrete elliptic operator

  We use a standard five point stencil. We use the grid point $M_{i,j}$ and its nearest neighbors in each direction: interface or grid points. More precisely, we denote u_S the value of the solution on the nearest point in the south direction, with coordinates (x_S, y_S). Similarly, we define u_N, u_W and u_E

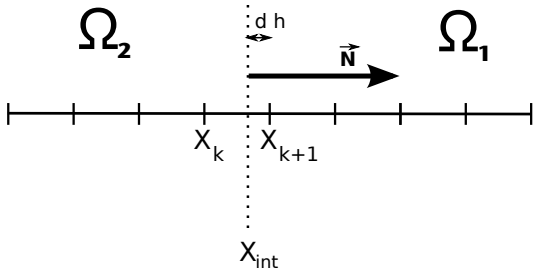

Figure 4: Geometrical configuration near the interface in one dimension.

and the associated coordinates (x_N, y_N), (x_W, y_W) and (x_E, y_E). The discretization reads

$$-\Big(\nabla.(k\nabla u)\Big)_{i,j} = -k\frac{\dfrac{u_N-u_{ij}}{x_N-x_i}-\dfrac{u_{ij}-u_S}{x_i-x_S}}{\dfrac{x_N-x_S}{2}} - k\frac{\dfrac{u_E-u_{ij}}{y_E-y_j}-\dfrac{u_{ij}-u_W}{y_j-y_W}}{\dfrac{y_E-y_W}{2}}. \tag{9}$$

The truncation error of this discretization is second-order accurate if all the points involved are grid points, that is, on regular grid points, and first-order on irregular grid points.

- Discrete jump conditions across the interface

We discretize the jump conditions (2) and (3) at each interface point $I_{i,j,\gamma}$, with $\gamma = N,S,W,E$.

$$u^2_{i,j,\gamma} - u^1_{i,j,\gamma} = \alpha(I_{i,j,\gamma}), \tag{10}$$

$$k_2(\partial_n u^2)_{i,j,\gamma} - k_1(\partial_n u^1)_{i,j,\gamma} = \beta(I_{i,j,\gamma}). \tag{11}$$

The discretization of the normal derivatives depends of the local geometry of the interface. On Figure 5 one can observe the four cases that are met in practice on each side of the interface. The first intersection between the normal to the interface and the grid is located on a segment: either $[M_{i,j}, M_{i,j-1}]$, or $[M_{i,j-1}, M_{i+1,j-1}]$, or $[M_{i,j}, M_{i,j+1}]$, or $[M_{i,j+1}, M_{i+1,j+1}]$.

The discrete normal derivative is computed as the normal derivative of the linear interpolant of the numerical solution on the triangle composed of the interface point $I_{i,j,\gamma}$ and the aforementioned segment.

If we denote K this triangle, $a_1 = (x_1, y_1)$, $a_2 = (x_2, y_2)$ and $a_3 = (x_3, y_3)$ its vertices, and u_1, u_2 and u_3 the values on these vertices, the basis functions on the vertices for the linear interpolation write

$$\lambda_j(x,y) = \alpha_j x + \beta_j y + \gamma_j, \ j = 1,2,3,$$

with

$$\alpha_j = \frac{y_k - y_i}{(x_j-x_k)(y_j-y_i)-(x_j-x_i)(y_i-y_k)},$$

$$\beta_j = \frac{x_i - x_k}{(x_j-x_k)(y_j-y_i)-(x_j-x_i)(y_i-y_k)},$$

$$\gamma_j = \frac{x_k y_i - x_i y_k}{(x_j-x_k)(y_j-y_i)-(x_j-x_i)(y_i-y_k)},$$

(n_x, n_y) being an approximation of the vector normal to the interface at point $I_{i,j,\gamma}$. With these notations, the approximation of the normal derivative writes

$$(\partial_n u)_{i,j,\gamma} = (u_1\,\alpha_1 + u_2\,\alpha_2 + u_3\,\alpha_3)n_x + (u_1\,\beta_1 + u_2\,\beta_2 + u_3\,\beta_3)n_y.$$

This discretization is only first-order accurate because it is based on a linear interpolation.

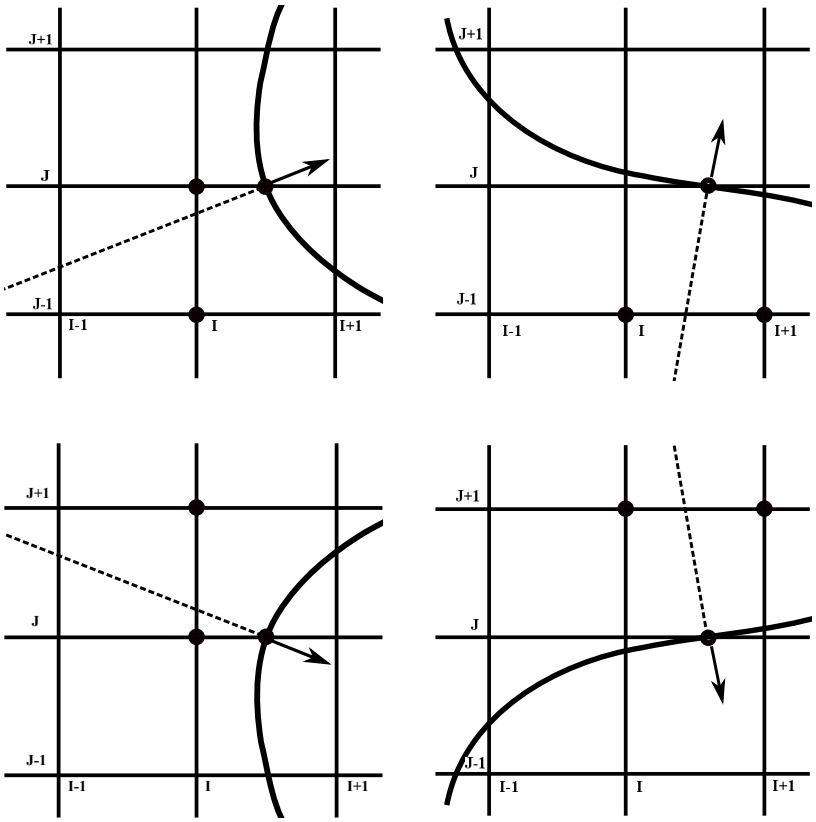

Figure 5: All possible stencils for the first-order flux discretization on the left side of the interface, with points involved in the discretization signaled by black circles.

2.4 Discretization matrix

In the following we will denote A_h the discretization matrix that we consider, in one or two dimensions. We replace the variable $u^2_{i,j,\gamma}$ by $u^1_{i,j,\gamma} + \alpha(I_{i,j,\gamma})$ in the equations (7) or (11), and (6) or (9), in order to eliminate the jump conditions (10) or (8) from the linear system. This does not change the truncation errors for these equations because the jump conditions (10) or (8) are exact. We rewrite the whole linear system by separating the array of interface unknowns ($\mathbf{u_{int}}$) from the array of grid unknowns ($\mathbf{u_g}$), and among these unknowns, the unknowns in the subdomain Ω_1 ($\mathbf{u^1_g}$) from the unknowns in the subdomain

Ω_2 ($\mathbf{u_g^2}$). This leads to

$$A_h\mathbf{u} = \left(\begin{array}{cc|cc} \Delta_1 & 0 & \Delta_{int}^1 & 0 \\ 0 & \Delta_2 & 0 & \Delta_{int}^2 \\ \hline F_1 & F_2 & F_{int}^1 & F_{int}^2 \end{array}\right) \left(\begin{array}{c} \mathbf{u_g^1} \\ \mathbf{u_g^2} \\ \hline \mathbf{u_{int}^1} \end{array}\right) = \left(\begin{array}{c} f_1+g_1(\alpha) \\ f_2+g_2(\alpha) \\ \beta+g_3(\alpha) \end{array}\right) = F,$$

with Δ_1 and Δ_{int}^1 (resp. Δ_2 and Δ_{int}^2) the blocks corresponding to the discretization on the elliptic operator on subdomain Ω_1 (Ω_2), F_1 and F_2, F_{int}^1 and F_{int}^2 accounting respectively for the contributions from grid points and interface points to the discretization of flux jump conditions (7) or (11). More precisely, the array $F_1\mathbf{u}_g^1 + F_{int}^1\mathbf{u}_{int}$ and $F_2\mathbf{u}_g^2 + F_{int}^2\mathbf{u}_{int}$ approximates respectively the values of $k_1\partial_n u^1$ and $-k_2\partial_n u^2$ on the interface points. The terms $g_i(\alpha)$, $i = 1,2,3$, account for the presence in the right-hand side of a term depending on $\alpha(I_{i,j,\gamma})$ because of the elimination of the variable $u_{i,j,\gamma}^2$.

The punctual error array $\mathbf{e}$ and the truncation error array τ obey the same linear relationship as the numerical solution and the source terms:

$$A_h\mathbf{e} = \tau,$$

or

$$\left(\begin{array}{cc|cc} \Delta_1 & 0 & \Delta_{int}^1 & 0 \\ 0 & \Delta_2 & 0 & \Delta_{int}^2 \\ \hline F_1 & F_2 & F_{int}^1 & F_{int}^2 \end{array}\right) \left(\begin{array}{c} e_g^1 \\ e_g^2 \\ \hline e_{int}^1 \end{array}\right) = \left(\begin{array}{c} \varepsilon_g^1 \\ \varepsilon_g^2 \\ \varepsilon_{int}^1 \end{array}\right).$$

3 Convergence proof in the two-dimensional case

The sketch of the convergence proof is the following: first we prove the monotonicity of the discretization matrix, then we use it to apply a discrete maximum principle to the matrix, thanks to which we obtain estimates on the coefficients of the inverse matrix, block by block.

3.1 Monotonicity of the discretization matrix

Here we aim to prove that A_h is monotone, that is, that all the coefficients of the inverse matrix of A_h are positive. Let $\mathbf{v}$ be an array of size $N^2 + N_{int}$, corresponding to N^2 grid points and N_{int} interface unknowns such that all coefficients of $A_h\mathbf{v}$ are positive, which we denote $A_h\mathbf{v} \geq 0$. We aim to prove that $\mathbf{v} \geq 0$, that is, that all coefficients of $\mathbf{v}$ are positive.

The first step is to remark that, if the minimum of $\mathbf{v}$ is located on an interface point, then with the notations of Figure 6 the left normal derivative (in Ω_1) at this interface point is negative and the right normal derivative (in Ω_2) at this interface point is positive. Indeed, the approximation of the normal derivative is constant, because it computed from a linear interpolation on a triangle, and its sign depends of the orientation of the normal to the interface. With the notations and orientation of the normal defined on Figure 6, if the minimum of $\mathbf{v}$ is located on the considered interface point, then the left normal derivative at this interface point is negative and the right normal derivative at this interface point is positive. Moreover, if the approximated normal derivative is zero, it means that the three points values involved in the stencil are equal.

Now we consider the smallest coefficient of $\mathbf{v}$ in the whole domain, interface points included. This coefficient can either be located on a grid point in one of the subdomains Ω_1 or Ω_2, or on an interface point.

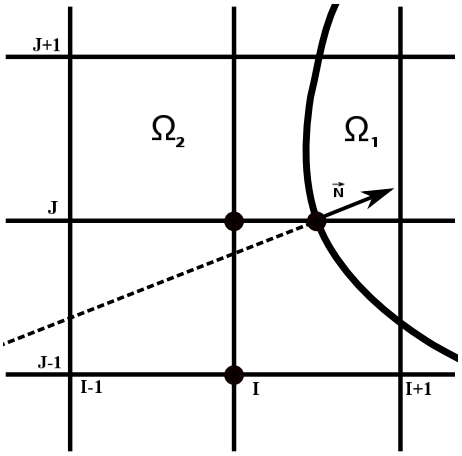

Figure 6: Geometrical configuration near the interface in two dimensions.

- If the minimum is located on one border of the computational domain

  We assume for instance that the minimum of $\mathbf{v}$ is $v_{1,j}$ with $j \in [2, N-1]$. The other cases would be treated the same way. The elliptic operator inequality on this grid point yields:

  $$\frac{4v_{1,j} - v_{2,j} - v_{1,j+1} - v_{1,j-1}}{h^2} \geq 0,$$

  then we have $4v_{1,j} \geq v_{2,j} + v_{1,j+1} + v_{1,j-1} \geq 3v_{1,j}$ and thus $v_{1,j} \geq 0$. Therefore all values of $\mathbf{v}$ are positive.

- If the minimum is reached on a grid point in one subdomain sharing at least one point with $\delta\Omega$

  In this case we denote (i_0, j_0) the indices of the smallest component of $\mathbf{v}$. We assume the grid point is a regular grid point (otherwise the formula would have slightly different weights, but the reasoning would be the same). Using the elliptic operator inequality on this point we can write:

  $$4v_{i_0,j_0} - v_{i_0+1,j_0} - v_{i_0-1,j_0} - v_{i_0,j_0+1} - v_{i_0,j_0-1} \geq 0,$$

  we deduce that $v_{i_0+1,j_0} = v_{i_0-1,j_0} = v_{i_0,j_0+1} = v_{i_0,j_0-1} = v_{i_0,j_0}$. Using similar inequalities of the elliptic operator in all the subdomain, we deduce that all values in the subdomain, including the boundary values, are equal to v_{i_0,j_0}. We use now the reasoning of the last paragraph to conclude that all values of $\mathbf{v}$ are positive.

- If the minimum is reached on a grid point in one subdomain which does not share any point with $\delta\Omega$

  We use the notations and geometrical configuration of Figure 4. We assume, without loss of generality, that the subdomain is Ω_1 and we denote (i_0, j_0) the indices of the smallest component of $\mathbf{v}$. We assume the grid point is a regular grid point (otherwise the formula would have slightly different weights, but the reasoning would be the same). Writing the elliptic operator inequality on this point, we obtain

  $$4v_{i_0,j_0} - v_{i_0+1,j_0} - v_{i_0-1,j_0} - v_{i_0,j_0+1} - v_{i_0,j_0-1} \geq 0,$$

  and we deduce that $v_{i_0+1,j_0} = v_{i_0-1,j_0} = v_{i_0,j_0+1} = v_{i_0,j_0-1} = v_{i_0,j_0}$. Using similar inequalities of the elliptic operator in all the subdomain, we deduce that all values in the subdomain, including the interface values, are equal to the minimum value v_{i_0,j_0}.

Let us consider one of these interface values. As noticed previously, the fact that all values are equal in the subdomain implies that the normal derivative at the interface point is zero. Due to the fact that $A_h v \geq 0$, we can write on this interface point:

$$0 = k^1(\partial_n v^1)_{i,j,\gamma} \quad \leq \quad k^2(\partial_n v^2)_{i,j,\gamma}.$$

On the other side, because the minimum value is reached on this interface point, we have also

$$(\partial_n v^2)_{i,j,\gamma} \geq 0.$$

Consequently, $(\partial_n v^1)_{i,j,\gamma} = (\partial_n v^2)_{i,j,\gamma} = 0$. Consequently the values of the grid points involved in the stencil for $(\partial_n v^2)_{i,j,\gamma}$ are equal to the value of the interface point. It means that there are two grid points in the subdomain Ω_2 where the minimum value is reached.

Now there are two possibilities: either the subdomain Ω_2 has a non-void intersection with $\delta\Omega$, and we can apply the reasoning of the last paragraph to conclude, or Ω_2 has a void intersection with $\delta\Omega$, and we apply again the reasoning of this paragraph, switching from subdomains to subdomains, until finding a subdomain whose intersection with $\delta\Omega$ is non empty.

- If the minimum is located on one interface point

  On this interface point, following the notations of Figure 4 we have the two relationships

$$\begin{aligned}(\partial_n v^2)_{i,j,\gamma} &\leq 0,\\ (\partial_n v^1)_{i,j,\gamma} &\geq 0.\end{aligned}$$

  Furthermore, we know that

$$k^2(\partial_n v^2)_{i,j,\gamma} - k^1(\partial_n v^1)_{i,j,\gamma} \quad \geq \quad 0.$$

  We infer from the previous inequalities that $(\partial_n v^2)_{i,j,\gamma} = (\partial_n v^1)_{i,j,\gamma} = 0$. Therefore there are at least two grid points in each subdomain where the minimum value is reached. We can then follow the reasoning of one of the two last paragraphs.

Finally, we conclude that all values of $\mathbf{v}$ are positive. Consequently the matrix A_h is monotone. As a corollary, A_h is invertible.

3.2 Notations and reminder of the method of Ciarlet

Here we recall the principle of the method presented in [7] to prove the convergence of finite-difference methods with a discrete maximum principle. We do not use exactly the same type of discretization matrix as in this reference, due to the different way to account for boundary conditions, so here we present the reasoning in the case of our discretization matrix.

In the following, the letters P and Q represent, depending of the context, either discretization points (on the grid or on the interface) or their indices in the global numerotation of the matrix. For instance, we denote $u(P)$ the coefficient of the row of u with the same index than the point P. Similarly, $(AU)(P)$ represents the coefficient of the P-th row of the array AU, and $A_h(P,Q)$ is the coefficient of the P-th row and Q-th column of the matrix A_h. We also define respectively by $A_h(:,Q)$ and $A_h(P,:)$ the Q-th column and the P-th row of the matrix A.

For each $Q \in \Omega_h$, define the discrete Green's function $G_h(P,Q)$ with $P \in \Omega_h$ as the solution of the discrete problem:

$$\left\{ \begin{array}{c} (A_h G_h)(P) = \left\{ \begin{array}{ll} 0, & P \neq Q \\ 1, & P = Q \end{array} \right. \quad P \in \Omega_h, \\ G_h(P) = 0, \quad P \in \delta\Omega_h. \end{array} \right. \tag{12}$$

In fact, each array $G_h(:,Q)$ represents a column of the inverse matrix A_h^{-1}. The matrix A_h being monotone, all values of $G_h(P,Q)$ are positive. With this definition of G_h we can write the solution of the numerical problem as a sum of the source terms of the linear system of subsection 2.4 multiplied by the local values of the discrete Green function:

$$u_h(P) = \sum_{Q\in\Omega_h} G_h(P,Q)\,(A_h u_h)(Q), \quad \forall P \in \Omega_h.$$

Now we present the result of [7], slightly modified to be adapted to our discretization matrix.

Theorem 1. *Let S be a subset of discretization points (thus corresponding also to a subset of the indices of the matrix), and W an array such that:*

$$\left\{ \begin{array}{c} W(P) \geq 0 \quad \forall P \in \Omega_h \cup \Sigma_h, \\ (A_h W)(P) \geq 0 \quad \forall P \in \Omega_h \cup \Sigma_h, \\ (A_h W)(P) \geq h^{-i} \quad \forall P \in S. \end{array} \right.$$

Then

$$\sum_{Q\in S} G_h(P,Q) \leq h^i W(P) \quad \forall P \in \Omega_h \cup \Sigma_h.$$

Proof. Using the definition of the discrete Green function, we can write

$$\Big(A_h \sum_{Q\in S} G_h(:,Q)\Big)(P) = \left\{ \begin{array}{ll} 1 & \text{if } P \notin S, \\ 0 & \text{if } P \in S. \end{array} \right.$$

Therefore,

$$A_h\Big(W - h^{-i}\sum_{Q\in S} G_h(:,Q)\Big)(P) \geq 0, \quad \forall P \in \Omega_h \cup \Sigma_h.$$

As all coefficients of the inverse of A_h are positive, it leads to

$$W(P) - h^{-i}\sum_{Q\in S} G_h(P,Q) \geq 0, \quad \forall P \in \Omega_h \cup \Sigma_h,$$

and finally we obtain an estimate of the coefficients of $\sum_{Q\in S} G_h(:,Q)$ in terms of the coefficients of W:

$$\sum_{Q\in S} G_h(P,Q) \leq h^i W(P), \quad \forall P \in \Omega_h \cup \Sigma_h.$$

■

3.3 Convergence

Here we aim to find appropriate arrays W in order to obtain estimates on the coefficients of the inverse matrix for the different kinds of discretization points.

- Estimates for coefficients of columns corresponding to regular grid points and interface points

  Let us denote M a point with coordinates (x_M, y_M). We define the function f as:

$$f(x_M, y_M) = B - e^{-A\varphi(x_M,y_M)},$$

with φ the level-set function defined as the signed distance to the interface, negative in Ω_2 and positive in Ω_1.

This function satisfies:

$$\partial_n f(x,y) = Ae^{-A\varphi} \underbrace{(\partial_x\varphi\, n_x + \partial_y\varphi\, n_y)}_{=1},$$
$$\text{and } -\Big(\nabla.(k\nabla f)\Big) = k\Big[A^2\Big(\underbrace{(\partial_x\varphi)^2 + (\partial_y\varphi)^2}_{=1}\Big) - A\nabla.(\nabla\varphi)\Big]e^{-A\varphi},$$

because of the relationship between the gradient of the level-set function and the normal to the interface (5).

We choose A and B such that $kA^2 - A\nabla.(k\nabla\varphi) \geq 1$ and $B - e^{-A||\varphi||_\infty} > 0$, with $||\varphi||_\infty = \max_\Omega |\varphi|$. Therefore,

$$k^2\partial_n f^2(x,y) - k^1\partial_n f^1(x,y) \geq (k^2 - k^1)Ae^{-A||\varphi||_\infty},$$
$$-\Delta f \geq e^{-A||\varphi||_\infty}.$$

The array W defined by $W(Q) = f(x_Q, y_Q)$ for all $Q \in \Omega_h \cup \Sigma_h$ has all its coefficient positive. Because the discretizations of the elliptic operator and the flux at the interface are consistent, the discrete versions of $-\nabla.(k\nabla f)$ and $\partial_n f$, discretized as presented in section 2, are also positive if h is small enough. Consequently, $(AW)(P) \geq 0$ for all indices $P \in \Omega_h \cup \Sigma_h$, and we can write

$$(AW)(P) \geq (k^2 - k^1)A\frac{e^{-A||\varphi||_\infty}}{2} \quad \forall P \in \Sigma_h,$$
$$(AW)(P) \geq \frac{e^{-A||\varphi||_\infty}}{2} \quad \forall P \in \Omega_h^{**}.$$

Following the result of Ciarlet, we have the following estimates:

$$\sum_{Q\in\Omega_h^{**}} G_h(:,Q) \leq \frac{2}{e^{-A||\varphi||_\infty}}, \tag{13}$$

$$\sum_{Q\in\Sigma_h} G_h(:,Q) \leq \frac{2}{e^{-A||\varphi||_\infty}(k^2 - k^1)A}. \tag{14}$$

- Estimates for coefficients of columns corresponding to irregular grid points

Let us assume first that we consider the set of irregular grid points on the Ω_2 side. We define the function f by :

$$f(x,y) = \begin{cases} B+1 & \text{if } (x,y) \in \Omega_2, \\ B - e^{-A\varphi(x,y)} & \text{if } (x,y) \in \Omega_1 \cup \Sigma, \end{cases}$$

with φ the level-set function defined previously as the signed distance to the interface, negative in Ω_2 and positive in Ω_1. This function satisfies:

$$\partial_n f(x,y) = \begin{cases} Ae^{-A\varphi} \underbrace{(\partial_x\varphi\, n_x + \partial_y\varphi\, n_y)}_{=1} \text{ for } (x,y) \in \Omega_1, \\ 0 \text{ for } (x,y) \in \Omega_2, \end{cases}$$

and

$$-\nabla.(k\nabla f)(x,y) = \begin{cases} \left(A^2 - A\Delta\varphi\right)e^{-A\varphi} \text{ for } (x,y) \in \Omega_1, \\ = 0 \text{ for } (x,y) \in \Omega_2 \cap \Omega_h^{**}, \\ \geq \frac{1}{h^2} \text{ for } (x,y) \in \Omega_2 \cap \Omega_h^{*}. \end{cases}$$

Again, we choose A and B such that $A^2 - A\Delta\varphi \geq 1$ and $B - e^{-A||\varphi||_\infty} > 0$. All the coefficients of the array W defined by $W(Q) = f(x_Q, y_Q)$ for all $Q \in \Omega_h \cup \Sigma_h$ are positive. Because the discretizations of the elliptic operator and the flux at the interface are consistent, the discrete versions of $-\nabla.(k\nabla f)$ and $\partial_n f$, discretized as presented in section 2, are also positive if h is small enough. Consequently, $(AW)(P) \geq 0$ for all indices P, and we can write more precisely:

$$(AW)(P) \geq \frac{1}{h^2} \text{ for all } P \in \Omega_2 \cap \Omega_h^*.$$

We deduce that

$$\sum_{Q \in \Omega_h^* \cap \Omega_2} G_h(:,Q) \leq h^2. \tag{15}$$

The same reasoning can be followed with the function

$$f(x_M, y_M) = \begin{cases} B+1 & \text{if } P \in \Omega_1, \\ B - e^{-A\varphi(x_M, y_M)} & \text{if } P \in \Omega_2 \cup \Sigma_h, \end{cases}$$

to obtain a similar estimate for irregular grid points in Ω_1

$$\sum_{Q \in \Omega_h^* \cap \Omega_1} G_h:,Q \leq h^2. \tag{16}$$

Finally, combining (13), (14), (15) and (16), we obtain an estimate of the local error on every point P in $\Omega_h \cup \Sigma_h$, with $\bar{u}$ the exact solution:

$$\begin{aligned} |\bar{u}(P) - u(P)| &= |\sum_{Q \in \Omega_h} G_h(P,Q)\tau(Q)|, \\ &\leq |\sum_{Q \in \Omega_h^{**}} G_h(P,Q)\tau(Q)| + |\sum_{Q \in \Omega_h^{*}} G_h(P,Q)\tau(Q)| + |\sum_{Q \in \Sigma_h} G_h(P,Q)\tau(Q)|, \\ &\leq \sum_{Q \in \Omega_h^{**}} G_h(P,Q)O(h^2) + \sum_{Q \in \Omega_h^{*}} G_h(P,Q)O(h) + \sum_{Q \in \Sigma_h} G_h(P,Q)O(h), \\ &\leq = O(h^2)O(1) + O(h)O(h^2) + O(h)O(1) = O(h). \end{aligned}$$

which proves that the numerical solution converges with first-order accuracy to the exact solution in L^∞-norm.

4 Convergence proof for the one-dimensional case

4.1 Monotonicy of the discretization matrix

Here we aim to prove that A_h is monotone, that is, that all the coefficients of the inverse matrix of A_h are positive, in spite of the fact that the matrix A is not diagonally-dominant in this one-dimensional case, due to the discretization terms near the interface.

Let $\mathbf{v}$ be an array of size $N + N_{int}$ corresponding to N grid points and N_{int} interface unknowns such that all coefficients of $A_h\mathbf{v}$ are positive. We begin by proving that, if the minimum of $\mathbf{v}$ is located on an

interface point x_{int} then, with the notations and orientation of the normal defined on Figure 4 then the left normal derivative at this interface point is negative and the right normal derivative at this interface point is positive. We use the notations defined on Figure 4 and we denote $v_{int} = \tilde{v}_{k,E}$.

Let us assume that the minimum of $\mathbf{v}$ is located on an interface point. The left normal derivative at x_{int} is discretized by

$$(\partial_n v^2)_{x_{int}} = \frac{3-2d}{(1-d)(2-d)h}(v_{int}-v_k) - \frac{1-d}{(2-d)h}(v_k - v_{k-1}).$$

By hypothesis $A_h\mathbf{v} \geq 0$ hence

$$\begin{aligned} -\Big(\frac{v_{int}-u_k}{(1-d)h} - \frac{v_k - v_{k-1}}{h}\Big) &\geq 0, \\ -(v_k - v_{k-1}) &\leq -\frac{(v_{int}-v_k)}{(1-d)}, \end{aligned}$$

therefore

$$\begin{aligned} (\partial_n v^2)_{x_{int}} &\leq \frac{3-2d}{(1-d)(2-d)h}(v_{int}-v_k) - \frac{1-d}{(1-d)(2-d)h}(v_{int}-v_k), \\ &\leq \frac{2-d}{(1-d)(2-d)h}(v_{int}-v_k) \leq 0. \end{aligned}$$

Moreover, if one can prove that the normal derivative is zero, with the last inequality we can deduce that $v_k = v_{int}$. Similarly, the right normal derivative at x_{int} is discretized by

$$(\partial_n v^1)_{x_{int}} = \frac{1+2d}{d(d+1)h}(u_{k+1}-v_{int}) - \frac{d}{(1+d)h}(v_{k+2}-v_{k+1}).$$

By hypothesis $A_h\mathbf{v} \geq 0$ hence

$$\begin{aligned} -\Big(\frac{v_{k+2}-v_{k+1}}{h} - \frac{v_{k+1}-v_{int}}{dh}\Big) &\geq 0, \\ -(v_{k+2}-v_{k+1}) &\geq -\frac{v_{k+1}-v_{int}}{d}, \end{aligned}$$

therefore

$$\begin{aligned} (\partial_n v^1)_{x_{int}} &\geq \frac{1+2d}{d(d+1)h}(v_{k+1}-v_{int}) - \frac{d}{d(1+d)h}(v_{k+1}-v_{int}), \\ &\geq \frac{1+d}{d(d+1)h}(v_{k+1}-v_{int}) \geq 0. \end{aligned}$$

If the normal derivative is zero, then $v_{k+1} = v_{int}$.

Once we have proven this property, the proof of monotonicity of the matrix is exactly the same as in two dimensions, so for the sake of brevity we do not re-write it.

4.2 Second-order convergence

With exactly the same reasoning than in subsection 3.3 we can prove the estimates (13), (14), (15) and (16). We use them to obtain an estimate of the local error on every point P in$\Omega_h \cup \Sigma_h$:

$$\begin{aligned}
|\bar{u}(P) - u_h(P)| &= |\sum_{Q\in\Omega_h} G_h(P,Q)\tau(Q)|, \\
&\leq |\sum_{Q\in\Omega_h^{**}} G_h(P,Q)\tau(Q)| + |\sum_{Q\in\Omega_h^{*}} G_h(P,Q)\tau(Q)| + |\sum_{Q\in\Sigma_h} G_h(P,Q)\tau(Q)|, \\
&\leq \sum_{Q\in\Omega_h^{**}} G_h(P,Q)O(h^2) + \sum_{Q\in\Omega_h^{*}} G_h(P,Q)O(h) + |\sum_{Q\in\Sigma_h} G_h(P,Q)O(h^2)|, \\
&\leq = O(h^2)O(1) + O(h)O(h^2) + O(h^2)O(1) = O(h^2),
\end{aligned}$$

which proves that the numerical solution converges with second-order accuracy to the exact solution in L^∞-norm.

5 Discussion

Numerous numerical methods have been developed for solving the problem (1) - (3), leading to various orders of accuracy for the convergence: the pioneering work of Mayo in 1984 [17], where an integral equation was derived to solve elliptic interface problems with piecewise coefficients to second order accuracy in maximum norm, the very well known Immersed Interface Method (IIM) LeVeque and Li (1994) [13] (second order accurate in maximum norm), and its developments, among them: the fast IIM algorithm of Li [14] for elliptic problems with piecewise constant coefficients, the Explicit Jump Immersed Interface Method (EJIIM) by Wiegmann and Bube [22], the Decomposed Immersed Interface Method (DIIM) by Bethelsen [3], and the MIIM (maximum principle preserving) by Li and Ito [15]. Another class of Cartesian method introduced by Zhou et al. is the Matched Interface and Boundary (MIB) method: [25], [24], [23]. This method can provide finite-difference schemes of arbitrary high order. The solution on each side of the interface is extended on fictitious points on the other side. These fictitious values are computed by iteratively enforcing the lowest order interface jump conditions. Finally, Chern and Shu [6] proposed a Coupling Interface Method, where the discretizations on each subdomain are coupled through a dimension by dimension approach using the jump conditions. All the methods cited above are second order accurate. Other classes of Cartesian methods also exist, only first order accurate for interface problems in the case of interface problems, but simpler to implement: Gibou et al. ([9], [10])

Concerning the discretization requirements needed to get a second-order spatial convergence, it has been noted since the introduction of Cartesian grid methods that a $O(h)$ truncation error at the points near the interface is enough to get a $O(h^2)$ convergence in maximum norm if the discretization is second-order on the regular grid points. However, in the literature, only few works have been devoted to the study of the second-order convergence of Cartesian grid methods for interface problems. For one-dimensional methods, Huang and Li performed in [11] a convergence analysis of the IIM, using non-negative comparison functions, and in [22] Wiegmann and Bube presented a proof of convergence for one-dimensional problems with piecewise constant coefficients, using a detailed analysis and identification of the coefficients of the matrices involved. In [12], a convergence proof was established in one-dimension for a variant of the method studied in this paper, applied in the context of electropermeabilization models. But this proof was based on a line by line analysis of the discretisation matrix, in order to obtain estimates of the coefficients of the inverse matrix. This technique would not be tractable in two dimensions, due to its complexity. For two-dimensional methods, Beale and Layton [1] proved in two-dimensions the second-order convergence for piecewise constant diffusion coefficients, using the fact that a grid function located near the interface can be written as the divergence of a function smaller in norm, and Li and Ito proved

in [15] the second-order convergence of their MIIM, using the maximum principle, but with a technical condition related to the location of the interface with respect to the grid point that is not always satisfied.

In this paper, the proof is also based on a discrete maximum principle. But its exact contents differs significantly from the proof in [15] because the discretization is not the same, for instance, due to the presence of interface unknowns, which make the monotonicity of the matrix a crucial step in the proof. To extend the result presented here to the second-order convergence in two dimensions, one would need to prove the monotonicity of the matrix, then the reasoning would be exactly the same as presented here. But this monotonicity property is not straightforward to prove, because of the second-order discretization of the fluxes near the interface. The strategy that was applied here in one dimension, that is, combining the flux inequalities with the elliptic operator inequalities on the grid points involved in the stencil of the numerical fluxes, does not seems convenient in two dimensions, and we probably have to find a different one.

6 Numerical validation

In this section we only provide numerical results for the first-order method in two dimensions. Indeed, the second-order method has already been validated in two-dimensions in [8], and consequently there is no need to show it in one dimension here. The following numerical results are not meant to assess good performances of the method or compare it to others methods of the literature, but simply to corroborate the analysis that we have performed.

In all the following test cases, we consider a square domain Ω consisting in the union of two subdomains Ω_1 and Ω_2 separated by an interface Σ. If not specified otherwise, $\Omega = [-1,1] \times [-1,1]$. We impose exact Dirichlet boundary conditions on the outer boundary of Ω.

6.1 Problem 1

It is a test case appearing in [25] (MIB method, case 3 of the tests on irregular interfaces) and [6] (CIM, example 4). We consider an elliptical interface Σ defined as:

$$(\frac{x}{18/27})^2 + (\frac{y}{10/27})^2 = 1.$$

The exact solution is:

$$u(x,y) = \begin{cases} e^x cos(y), \text{ inside } \Sigma, \\ 5e^{-x^2 - \frac{y^2}{2}} \text{ otherwise.} \end{cases}$$

As in [25] we fix the diffusion coefficient $k = 1$ outside the interface, and $k = 10$ inside the interface. We observe a first-order convergence, as presented in Table 1.

N	L^∞ error	order
20	1.2497×10^{-1}	-
40	$5.83079213 \times 10^{-2}$	1.10
80	3.0542764×10^{-2}	1.02
160	1.3751638×10^{-2}	1.06
320	$7.12846725 \times 10^{-3}$	1.03

Table 1: Numericals results for Problem 1.

6.2 Problem 2

It is a test case studied in [16]. We consider an spherical interface Σ defined by $r^2 = 1/4$ with $r = \sqrt{x^2+y^2}$. The exact solution is:

$$u(x,y) = \begin{cases} e^x \cos(y) \text{ inside } \Sigma \\ 0 \text{ otherwise,} \end{cases}$$

The numerical results and orders of convergence are presented in Table 2. We observe again a first-order convergence.

N	L^∞ error	order
20	4.9234×10^{-3}	-
40	2.2717×10^{-3}	1.12
80	1.0763×10^{-3}	1.10
160	5.5813×10^{-4}	1.05
320	2.4518×10^{-4}	1.08

Table 2: Numericals results for Problem 2.

References

[1] J. T. Beale and A. T. Layton. On the accuracy of finite difference methods for elliptic problems with interfaces. *Commun. Appl. Math. Comput. Sci.*, 1:91–119, 2006.

[2] M. Bergmann, F. Luddens, and L. Weynans. A sharp cartesian method for the simulation of air-water interface. In *Proceedings of the Eigth Eigth International Conference on Computational Fluid Dynamics, Chengdu, China*, 2014.

[3] P. Bethelsen. A decomposed immersed interface method for variable coefficient elliptic equations with non-smooth and discontinuous solutions. *J. Comput. Phys.*, 197:364–386, 2004.

[4] D. Bresch, T. Colin, E. Grenier, B. Ribba, and O. Saut. Computational modeling of solid tumor growth: the avascular stage. *SIAM J. Sci. Comput.*, 32:2321–2344, 2009.

[5] F. Buret, N. Faure, L. Nicolas, R. Perussel, and C. Poignard. Numerical studies on the effect of electric pulses on an egg-shaped cell with a spherical nucleus. Technical Report 7270, INRIA, 2010.

[6] I. Chern and Y.-C. Shu. A coupling interface method for elliptic interface problems. *J. Comput. Phys.*, 225:2138–2174, 2007.

[7] P. G. Ciarlet. Discrete maximum principle for finite-difference operators. *aequationes mathematicae*, 4:338–352, 1970.

[8] M. Cisternino and L. Weynans. A parallel second order cartesian method for elliptic interface problems. *Commun. Comput. Phys.*, 12:1562–1587, 2012.

[9] F. Gibou, R. P. Fedkiw, L.T. Cheng, and M. Kang. A second order accurate symmetric discretization of the poisson equation on irregular domains. *J. Comput. Phys.*, 176:205–227, 2002.

[10] F. Gibou and R.P. Fedkiw. A fourth order accurate discretization for the laplace and heat equations on arbitrary domains, with applications to the stefan problem. *J. Comput. Phys.*, 202:577–601, 2005.

[11] H. Huang and Z. Li. Convergence analysis of the immersed interface method. *IMA J. Numer. Anal.*, 19:583–608, 1999.

[12] O. Kavian, M. Leguebe, C. Poignard, and L. Weynans. Classical electropermeabilization modelling at the cell scale. *J. Math. Biol.*, 68:235–265, 2014.

[13] R. J. Leveque and L.Z. Li. The immersed interface method for elliptic equations with discontinuous coefficients and singular sources. *SIAM Numerical Analysis*, 31(4):1019–1044, 1994.

[14] Z.L. Li. A fast iterative algorithm for elliptic interface problems. *SIAM J. Numer. Anal.*, 35:230–254, 1998.

[15] Z.L. Li and K. Ito. Maximum principle preserving schemes for interface problems with discontinuous coefficients. *SIAM J. Sci. Comput.*, 23:339–361, 2001.

[16] X.-D. Liu, R. Fedkiw, and M. Kang. A boundary condition capturing method for poisson's equation on irregular domains. *J. Comput. Phys.*, 160:151–178, 2000.

[17] A. Mayo. The fast solution of poisson's and the biharmonic equations on general regions. *SIAM J. Numer. Anal.*, 21:285–299, 1984.

[18] S. Osher and R. Fedkiw. *Level Set Methods and Dynamic Implicit Surfaces*. Springer, 2003.

[19] S. Osher and J. A. Sethian. Fronts propagating with curvature-dependent speed: Algorithms based on hamilton-jacobi formulations. *J. Comput. Phys.*, 79(12), 1988.

[20] J. A. Sethian. *Level Set Methods and Fast Marching Methods*. Cambridge University Press, Cambridge, UK, 1999.

[21] J. A. Sethian. Evolution, implementation, and application of level set and fast marching methods for advancing fronts. *J. Comput. Phys.*, 169:503–555, 2001.

[22] A. Wiegmann and K. Bube. The explicit jump immersed interface method: finite difference method for pdes with piecewise smooth solutions. *SIAM J. Numer. Anal.*, 37(3):827–862, 2000.

[23] S. a Yu and G.W. Wei. Three-dimensional matched interface and boundary (mib) method for treating geometric singularities. *J. Comput. Phys.*, 227:602–632, 2007.

[24] Y. C. Zhou and G. W. Wei. On the fictitious-domain and interpolation formulations of the matched interface and boundary (mib) method. *J. Comput. Phys.*, 219:228–246, 2006.

[25] Y. C. Zhou, S. Zhao, M. Feig, and G. W. Wei. High order matched interface and boundary method for elliptic equations with discontinuous coefficients and singular sources. *J. Comput. Phys.*, 213:1–30, 2006.

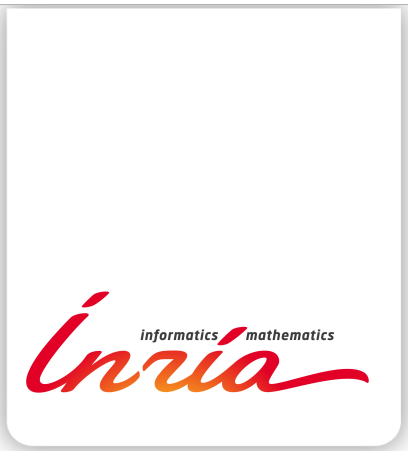

RESEARCH CENTRE
BORDEAUX – SUD-OUEST

351, Cours de la Libération
Bâtiment A 29
33405 Talence Cedex

Publisher
Inria
Domaine de Voluceau - Rocquencourt
BP 105 - 78153 Le Chesnay Cedex
inria.fr

ISSN 0249-6399